Sensors & Actuators: B. Chemical 270 (2018) 396–404

Contents lists available at ScienceDirect

Sensors and Actuators B: Chemical

journal homepage: www.elsevier.com/locate/snb

Phenotyping antibiotic resistance with single-cell resolution for the detection of heteroresistance

Fengjiao Lyu[a], Ming Pan[b], Sunita Patil[c], Jing-Hung Wang[d], A.C. Matin[d], Jason R. Andrews[c], Sindy K.Y. Tang[a,*]

[a] Department of Mechanical Engineering, School of Engineering, Stanford University, United States
[b] Department of Material Science and Engineering, School of Engineering, Stanford University, United States
[c] Division of Infectious Diseases and Geographic Medicine, School of Medicine, Stanford University, United States
[d] Department of Microbiology & Immunology, Stanford School of Medicine, Stanford University, United States

ARTICLE INFO

Keywords:
Droplet microfluidics
Antibiotic resistance
Heteroresistance
Single cell

ABSTRACT

Antibiotic resistance has emerged as an imminent threat to public health. It is also increasingly recognized to be a heterogeneous phenomenon: a population of bacteria, found *in vivo* or *in vitro*, often consists of a mixture of cells that have different degrees of resistance to antibiotics. The conventional metric to measure antibiotic resistance based on an ensemble-average minimum inhibitory concentration (MIC) fails to characterize the heterogeneity present within a bacterial population. This work describes a droplet microfluidics method to encapsulate single cells from a population consisting of a mixture of antibiotic-sensitive and antibiotic-resistant bacteria. Co-encapsulating viability probe alamarBlue with the cells allows the use of fluorescent drops as a read-out for drops that contain live cells after their exposure to antibiotics. Enumerating the fluorescent drops thus gives the number of resistant cells in the population. Our method enables the quantitative phenotyping of heterogeneous resistance, or heteroresistance, with single-cell resolution. We show that it is possible to detect a resistant sub-population that comprises as low as 10^{-6} of the entire population of cells. Such high resolution further allows us to measure the evolution of heteroresistance arising from the exposure of a homogeneous isogenic culture of susceptible cells to sub-lethal dosages of antibiotics. We demonstrate an application of this system to characterize genetic determinants of antimicrobial resistance emergence. The high resolution of phenotypic detection and quantification of minority variants demonstrated in this work has the potential to facilitate the elucidation of the mechanisms underlying heteroresistance. Such understanding will in turn inform the best practices for antibiotic use and containment of antimicrobial resistance in a wide range of settings from agriculture and aquaculture to disease management. Clinically, the ability to quantify and track the composition of a bacterial population will benefit the decision-making process in both the diagnosis and the treatment of bacterial infections, and will ultimately improve patient outcome and avert the spread of resistant populations.

1. Introduction

The evolution and spread of antibiotic resistance (ABR) in pathogens is emerging as a global threat to public health. In the U.S., more than 2 million people are infected with antibiotic-resistant bacteria each year [1]. At least 23,000 people in the U.S. die each year as a result of these infections [1]. The Centers for Disease Control and Prevention and the World Health Organization have called for urgent global action to combat ABR. The early detection of ABR has been identified as the key to effective treatment. Early detection of ABR has been challenging, however. Among many factors, a small sub-population (in some cases $< 10^{-3}$) of bacterial cells can exhibit resistance to antibiotics, which is below the limit of detection of standard drug susceptibility assays [2]. Failure to detect this sub-population can compromise treatment efficacy due to the persistence of the resistant sub-population, which may be selected for and preferentially grow in the setting of antimicrobial therapy, leading to the expansion and potential spread of resistant bacteria.

This heterogeneous resistance within a population of bacteria is referred to as heteroresistance, and has been reported in a wide range of micro-organisms, including *E. coli*, *S. aureus*, and *M. tuberculosis* [3]. The frequency of heteroresistance varies across different species, but is believed to be approximately equal to the normal rate of mutation, which is about one sub-clone in every 10^4–10^6 colonies [4].

* Corresponding author.
E-mail address: sindy@stanford.edu (S.K.Y. Tang).

https://doi.org/10.1016/j.snb.2018.05.047
Received 8 February 2018; Received in revised form 19 April 2018; Accepted 10 May 2018
Available online 14 May 2018
0925-4005/

Heteroresistance can arise from other factors. In particular, the exposure of bacteria to sub-lethal dosage of antibiotics has been found to play an important role [5,6]. Sub-lethal concentrations of antibiotics can occur both *in vivo* and in external environment. For *in vivo* conditions, factors such as inappropriate dosing regimen, poor patient adherence, poor drug pharmacological kinetics, and the presence of biofilms or other areas with limited antibiotic penetration can lead to a local environment where the antibiotic concentration is lower than the lethal level. In external environments, the use of antibiotics as feed additives to promote animal growth and production in agriculture and aquaculture, pollution from drug-production plants, excretion from humans and animals administered with antibiotics ending up in rivers, lakes, soils and even food products such as milk and meat can all lead to sub-lethal concentrations of antibiotics [6,7].

Exposure to sub-lethal dosage of antibiotics is found to have two basic effects. The first effect is the selection of pre-existing resistant sub-population from a population having a mixture of susceptible and resistant cells. Previous work has shown that antibiotics present at concentrations far below the minimum inhibitory concentration (MIC) reduced the exponential growth rate of the susceptible bacteria without apparent effect on the resistant bacteria, thereby enriching the resistant sub-population [8]. The second effect is the increase in mutation rate in an initially susceptible strain. In some cases, the increased formation of reactive oxygen species (ROS) due to sub-lethal antibiotic treatment has been found to increase the formation of a range of mutations, and in turn increases multidrug resistance and the emergence of heteroresistance [5,9,10]. In one study, it was found that the exposure to sub-MIC dosage of ampicillin for 2 days led to >1.5 fold increase in the MIC for multiple drugs including ampicillin, kanamycin, and tetracycline [5].

A variety of methods have been developed to detect antibiotic resistance and have been reviewed elsewhere [11–18]. For determining heteroresistance, the conventional method is the population analysis profiling (PAP) method [3]. A bacteria population, typically spread on a plate, is exposed to a gradient of antibiotic concentration. The growth of bacteria is measured at different concentrations following a procedure similar to that used to identify the MIC. Heteroresistance was considered to occur when the antibiotic concentration having the highest inhibitory effect was 8-fold or more higher than the highest non-inhibitory concentration [19]. This method cannot easily quantify the proportion of cells that are resistant among the population of cells, however. Previously, phenotypic culture-based drug susceptibility testing allowed the detection of resistant cells that comprise 10^{-2} of a population containing a mixture of isoniazid-resistant and isoniazid-susceptible *M. tuberculosis* strains [20]. This method is both slow and insensitive for detecting resistant sub-populations that comprise less than 10^{-2} of the population. Nucleic acid-based methods including polymerase chain reaction (PCR) gene detection have also been used to detect DNA sequences that are known to confer resistance. The resolution of these tests can be worse than that of phenotypic tests, however. For example, recent studies reported that line probe assay, real-time PCR, and sequencing failed to detect clinically relevant 10^{-2} portion of resistant *M. tuberculosis* [20]. Digital PCR has an improved performance but it was still limited to 10^{-3}, and it requires knowledge of resistant genes [21].

A key challenge in the detection of heteroresistance is, therefore, the lack of a method that offers sufficient resolution and sensitivity for the early detection of heteroresistance, which is critical for preventing the emergence of fully resistant strains [3,4,22,23]. Fundamentally, such method is also essential to the elucidation of the mechanisms underlying the emergence and evolution of the phenomena. At present, many mechanisms of antibiotic resistance remain unknown, with novel mechanisms being reported regularly in the literature. While many mutations contributing to antibiotic resistance have been identified, the relationship between the mutations and the phenotypic effects is complex, and has yet to be fully elucidated [24,25]. Importantly, in some cases of heteroresistance, the resistant and susceptible sub-populations are genetically identical, possibly arising from epigenetic changes [2,26]. On the other hand, phenotypic resistance detection is mechanistically agnostic, as it does not require prior knowledge of genomic determinants. In addition, it has been pointed out that the value of high-throughput genotyping is limited unless combined with high-throughput phenotyping [25].

As such, this work focuses on phenotyping instead of genotyping resistance. We describe a microfluidic method for the quantification of phenotypic heteroresistance by encapsulating single bacterial cells from a heterogeneous population into microfluidic droplets. We demonstrate the detection of resistant cells down to 10^{-6} of the whole population. We further show the use of our method for measuring the emergence of heteroresistance and the distribution of bacteria with different MIC when cells are subject to sub-lethal dosage of antibiotics. While some prior work has described the use of droplet microfluidics for detecting antibiotic resistance,[12–18] our results are new in the application of the method for quantifying the emergence of heteroresistance arising from the exposure of cells to a sub-lethal dosage of antibiotics.

2. Materials and methods

2.1. Synthesis of 60 nm F-SiO_2 NPs

We added 7.14 mL of tetraethyl orthosilicate (98%, Sigma-Aldrich) into a solution mixture containing 100 mL of ethanol (99%, Sigma-Aldrich), 2 mL of deionized water, and 2.86 mL of ammonium hydroxide solution (28 wt%, Sigma-Aldrich). The solution was stirred vigorously (~800 rpm) at room temperature overnight. 1 mL of *1H,1H,2H,2H*-Perfluorooctyltriethoxysilane (98%, Sigma-Aldrich) was then added directly to every 10 mL of the synthesized SiO_2 nanoparticles (NPs) dispersion obtained above, followed by vigorous stirring (~800 rpm) at room temperature for 6 h. Ethanol was added to dilute the reacting solution and terminate the reaction with a dilution factor of 5. Nanoparticles were then collected by centrifugation (Sorvall LEGEND X1R) at 5000 rpm for 60 min and removal of the supernatant. The solid particles were isolated by desiccation overnight. Further details were published in our previous work [27].

2.2. Bacterial strain, antibiotics, and fluorogenic probe

We used two strains of *E. coli* as our model bacteria for Figs. 2–5: one strain was resistant to ampicillin “AmpR” (ATCC 35218) and the other one was susceptible to ampicillin “AmpS” (ATCC 25922). For Fig. 6, we used wildtype E. coli strain “WT” (K-12 BW25113) and its isogenic *rpoS* deletion mutant “*ΔrpoS*”.[28]

We used ampicillin (Alfa Aesar) as the model antibiotic for Figs. 2–4, norfloxacin (Chem-Impex Int’l Inc.), kanamycin (bioWORLD), and tetracycline (Sigma-Aldrich) as model antibiotics for Fig. 5, and ampicillin, norfloxacin, and kanamycin as model antibiotics for Fig. 6. For Figs. 2 and 3, the concentration of ampicillin was fixed at 50 μg/mL in Luria-Bertani (LB) broth. For Fig. 4, we exposed AmpS to different concentrations of ampicillin as listed in the text to test our method of measuring heteroresistance arising from the exposure of cells to sub-lethal dosage of antibiotics. For Fig. 4a, the concentration of ampicillin inside droplets was fixed at 5 μg/mL. For Fig. 5, we exposed AmpS to 1 μg/mL ampicillin for 5 days before measuring heteroresistance to norfloxacin, kanamycin, and tetracycline. For Figs. 4b and 5, the concentrations of antibiotics used in droplets for the identification of MIC were listed in Table S1. For Fig. 6, we exposed WT and *ΔrpoS* to 1 μg/mL ampicillin and measured their heteroresistance to ampicillin, norfloxacin, and kanamycin, respectively, with the antibiotic concentrations listed in the figure.

We used alamarBlue as our fluorogenic probe. AlamarBlue is a cell viability indicator that is converted into a bright fluorescent product by metabolically active cells. The fluorescence evolution of alamarBlue

indicates cellular metabolic activity, and has been used previously for the detection of live cells [12,13,29].

2.3. Cell culture

For Figs. 2 and 3, we cultured cells in LB broth until OD_{600} reached a value of 0.5. The cells were then diluted to different concentrations for subsequent experiments. For Fig. 2, the concentrations of both AmpS and AmpR were 10^6 cfu/mL. For Fig. 3, different volumes of AmpR and AmpS were mixed to generate populations of cells to give a final ratio of [AmpS]/[AmpR] = 10^6, 10^5, 10^4, 10^3, 10^2, 10, and 1. The total bacteria concentration was fixed at 10^7 cfu/mL for [AmpS]/[AmpR] = 10^6 to 10, and at 10^6 cfu/mL for [AmpS]/[AmpR] = 1.

2.4. Device fabrication

We fabricated microchannels in poly(dimethylsiloxane) (PDMS) using soft lithography [30]. Inlets and outlets of the microchannels were punched using a biopsy puncher (Harris Uni-Core, outer diameter 1.20 mm). To fabricate on-chip electrodes, we heated the device at 200 °C and injected indium (99.99%) into the channels. Details of this method can be found elsewhere [31]. After cooling to room temperature, we rendered the channels hydrophobic by treatment with Aquapel (Pittsburgh, PA).

2.5. Droplet generation and single cell encapsulation with antibiotics

We generated monodisperse droplets using a flow-focusing nozzle (Fig. 1).[32] The continuous phase was HFE-7500 (3 M, St. Paul, MN) containing 60 nm F-SiO_2 NPs at a concentration of 6% (wt/wt) [27,33,34]. We mixed the disperse phases on-chip by introducing two separate aqueous streams: one contained bacteria mixture in LB, and the other one contained antibiotic in LB at various concentrations. The two streams came into contact ~1 mm upstream of the flow-focusing nozzle. The flow rates of the continuous phase and the two streams of dispersed phase were fixed at 0.5, 0.1 and 0.1 mL/h, respectively. All droplets were generated at room temperature at a rate of ~740 drops/second for a single nozzle. The average droplet volume was approximately 75 pL. The standard deviation of droplet volume is < 3% of the average droplet volume. Based on Poisson distribution [35–41], approximately 96.3% of the drops that contained cells contained a single cell (see details in Fig. S1). After generation, the droplets were collected into a 1.5 mL Eppendorf tube and incubated at 37 °C with shaking at 225 rpm off-chip for 1 h to allow the antibiotic to take effect on the cells (Fig. S2).

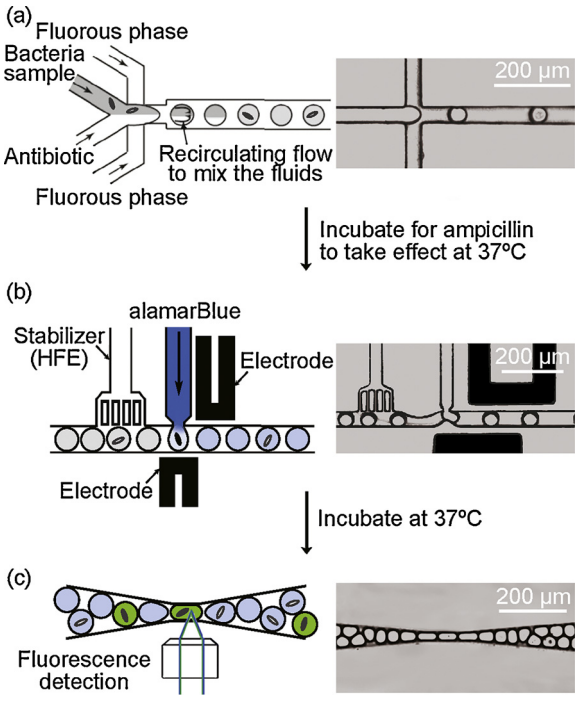

Fig. 1. Scheme and optical images of the microfluidic process flow. The process consists of three main parts: (a) droplet generation and encapsulation of bacteria with antibiotic, (b) pico-injection of alamarBlue into droplets, and (c) the detection of fluorescence from the drops.

2.6. Pico-injection of alamarBlue

After incubation with antibiotic, the droplets were reinjected into a microfluidic channel where alamarBlue was pico-injected into each drop at room temperature [42,43]. The pico-injected solution contained the as-purchased alamarBlue solution (Thermo Fisher, DAL1025). The final concentration of alamarBlue in the pico-injected droplet was approximately 1/8 of that of the as-purchased alamarBlue solution. For the results in Fig. 2 only, the pico-injected solution also contained 200 μM fluorescein as an internal reference to account for the non-uniform spatial distribution of light intensity under the microscope we used. The final concentration of fluorescein in the pico-injected droplet was approximately 25 μM. Extra continuous phase was injected upstream of the pico-injector through a pressure stabilizer to space the droplets and to improve the stability of the pico-injection process [43,44]. We applied constant pressure using a compressed air source to drive the flow of the continuous phase through the pressure stabilizer (345 mbar) and alamarBlue through the pico-injector (200 mbar). To trigger pico-injection, we applied a pulsating DC voltage that varied between 0 and 100 V at 5 kHz. The reinjection rate of the drops was 0.35 mL/h. The pico-injection rate was about 800 drops/second, and the pico-injected volume was about 10 pL (Fig. S3). The pico-injected droplets were then collected into 1 mL-syringe (Monoject) and incubated at 37 °C off-chip for ~2 h. We have verified that alamarBlue turned on at a similar rate with or without shaking in this step.

2.7. Imaging of drops and enumeration of fluorescent drops

For Fig. 2, the drops were reinjected into a PDMS well with a height of 30 μm. Fluorescence images were subsequently obtained by a 10 x microscope objective in an inverted optical microscope coupled with an Electron Multiplying Charge Coupled Device (EMCCD) camera (Andor Technology, South Windsor, CT). For Fig. 2 only, we normalized all intensity from alamarBlue ($I_{measured}$) by the intensity of fluorescein ($I_{reference}$) in the same droplet: $I_{normalized} = I_{measured}/I_{reference}$. Normalization was needed here as the excitation light from the microscope was not uniform throughout the field of view.

For the enumeration of fluorescent drops (Figs. 3–6), we reinjected the drops into a tapered channel consisting of a narrow constriction with a cross section of 30 μm x 30 μm at a flow rate of 0.6 mL/h. The volume fraction of the reinjected drops was about 80%. The throughput for droplet detection was ~1600 droplets/sec. The width of the constriction (30 μm) was less than one droplet diameter (~52 μm) to ensure the droplets pass through the constriction one at a time. Excitation light from a UV lamp was focused onto the constriction using a 40 x microscope objective in an inverted microscope (Nikon Eclipse TE2000). The fluorescence from the drops was collected from the same objective through an emission filter into a photomultiplier tube "PMT" (Hamamatsu product number: 56420001). A gain of 13 V was applied to the PMT. We automated the recoding of PMT output voltages with a custom LabView script. A voltage peak above the threshold value was identified as a fluorescent drop. We quantified the number of fluorescent drops by counting the number of voltage peaks above the threshold value. To set the threshold voltage (V_{th}) to differentiate a fluorescent drop from a non-fluorescent drop, we first measured the

mean ($\overline{V}_{\text{negative}}$) and the standard deviation (σ) in voltage from drops without bacteria ("negative drops"). A threshold value was then set at $V_{\text{th}} = \overline{V}_{\text{negative}} + n\sigma$. A value of $n = 6$ was used such that less than $1 - \text{erf}\left(\frac{n}{\sqrt{2}}\right) = 1.97 \times 10^{-9}$ of the negative drops had a value exceeding V_{th}. Voltage peaks with values $V > V_{\text{th}}$ were counted as a fluorescent drop.

2.8. Measurement of heteroresistance after treating of cells to sub-lethal dosage of antibiotics

For Figs. 4 and 5, one untreated AmpS colony was inoculated in 2 mL of LB broth and cultured overnight. We determined the MIC of the culture and diluted the culture 1:1000 into another 2 mL of LB broth containing different concentrations of ampicillin as listed in the text. This culture was then grown at 37 °C by applying continuous shaking at 225 rpm for 1 day. On each day for the following days, we repeated the dilution and incubation process above. We measured the MIC of the culture at the end of each day during the multi-day ampicillin treatment.

For the measurement of MIC in droplets, aliquots of either the untreated culture or the culture after different days of ampicillin treatment were diluted to 2×10^6 cfu/mL with LB. The diluted culture (containing a diluted concentration of ampicillin ~ 10^{-3} μg/mL) was used as one of the disperse phases to generate droplets with different concentrations of antibiotics. For Fig. 4a, the concentration of ampicillin used in droplets was 5 μg/mL. For Figs. 4b and 5, the concentrations of antibiotics inside the droplets for the identification of MIC were listed in Table S1. After generation, the droplets were collected into 1.5 mL Eppendorf tube for 1-h incubation at 37 °C (225 rpm), followed by pico-injection of alamarBlue and enumerating fluorescent drops as described above. The MIC for each single cell was determined as the lowest antibiotic concentration that inhibited an increase in fluorescence of alamarBlue and resulted in a detected voltage lower than the threshold voltage (V_{th}) as acquired by the PMT.

For the measurement of the ensemble-average MIC, we followed a standard protocol published previously [45]. Aliquots of either the untreated or treated culture were diluted 1:1000 into 2 mL LB containing different concentrations of antibiotics (listed in Table S1). The resulting samples were then grown at 37 °C with continuous shaking at 225 rpm for 20 h. The OD_{600} of each culture was measured by Thermo Scientific NanoDrop 1000 Spectrophotometer. The ensemble-average MIC was then determined by the lowest concentration that inhibited > 90% of bacteria growth based on OD_{600} [5].

For Fig. 6(i) and (ii), we cultured one untreated WT colony and one untreated *ΔrpoS* colony in LB with 1 μg/mL ampicillin respectively, and measured their ensemble-average MIC and MIC in droplets, using the methods described above.

3. Results and discussion

3.1. Design and process flow of the droplet microfluidics method for measuring heteroresistance

Fig. 1 shows the general process flow of our microfluidic method to detect heteroresistance. Antibiotic (ampicillin) was mixed with the bacteria sample immediately before droplet generation. By using a sufficiently low bacterial concentration, we were able to encapsulate single cells into droplets as governed by Poisson distribution [35]. The drops were then incubated for antibiotics to take effect. Cell viability indicator, alamarBlue, was subsequently pico-injected into each drop. After incubation, the presence of live cells in the drops increased the fluorescence of alamarBlue and rendered the droplet fluorescent. Counting the number of fluorescent drops gave the number of viable cells that were resistant to antibiotics. Here, the encapsulation of cells into drops before the incubation with antibiotics was critical to preserve the ratio of resistant cells to susceptible cells in the original sample. If we had incubated the cells with antibiotics in bulk solution prior to the encapsulation into drops, resistant cells could grow preferentially over susceptible cells, thereby increasing the ratio of resistant cells to susceptible cells from that in the original sample.

We introduced alamarBlue after the cells were incubated with antibiotics to increase the contrast in fluorescence signal between droplets containing resistant cells and susceptible cells. Since it took a finite amount of time for ampicillin to take effect, susceptible cells would be able to increase the fluorescence of alamarBlue if it is introduced at the same time as ampicillin to the cells. In our system, we found that it was sufficient to incubate cells with ampicillin for 1 h before introducing alamarBlue to the cells in order to distinguish the resistant cells (AmpR) from the sensitive cells (AmpS) (Fig. S2). Depending on the specific strain of the bacteria and antibiotics used, the incubation time with antibiotics would vary. Separating the incubation step with antibiotics from the incubation step with alamarBlue allows the incubation times to be customized for different combinations of cells and antibiotics used. In addition, we have chosen to use amphiphilic nanoparticles instead of conventional surfactants to stabilize the drops here, as alamarBlue was known to leak from surfactant-stabilized drops into other drops [46]. Such leakage would cause undesirable crosstalk of droplet content and would destroy the accuracy of the assay. We have shown previously that replacing surfactants with nanoparticles mitigated such leakage [27,33,34]. Furthermore, the nanoparticles were shown previously to be biocompatible and did not change the growth of *E. coli* and other bacteria in drops stabilized by the particles [47].

3.2. Identification of alamarBlue incubation time

To identify the appropriate incubation time of cells with alamarBlue, we sampled the drops at various time points. Fig. 2 shows the distribution of alamarBlue fluorescence from the drops generated from a mixture of AmpS and AmpR cells at a ratio of [AmpS]:[AmpR] = 1:1 as a function of incubation time with alamarBlue. At time t = 0, all drops were dark. As the time of incubation increased, two populations of drops – one with increased intensity and one at the same intensity as those at t = 0 – started to emerge. The population with increased intensity corresponded to drops containing AmpR. The population with a low intensity (approximately the same intensity as that at t = 0) corresponded to drops that contained either no cells or AmpS. At t = 2 h, the fluorescence intensity of drops containing AmpR can be distinguished from that of drops without AmpR. We thus chose to use 2 h as the minimum incubation time with alamarBlue for all subsequent experiments.

Although the main purpose of this figure was to identify the time for incubation with alamarBlue, we note that the proportion of fluorescent drops measured matched our expectations based on the Poisson encapsulation process.[35] The percentages of drops with normalized fluorescence intensity > 1.5 were 3.64%, 3.59%, 3.83%, 3.49%, 3.56% at t = 2, 3, 4, 5 and 15 h, respectively. Given the volume of the drop (75 pL), and the bacteria concentration (10^6 cfu/mL) used, we expect an average of 0.075 cells per drop. As the encapsulation process follows Poisson statistics, the proportion of drops with cells was approximately 7.2%. Since [AmpS]:[AmpR] = 1:1 here, the expected percentage of fluorescent drops was 3.6% of the population of drops examined. This value was close to those measured. The small variations were likely due to the relatively small number of drops sampled here (~600 drops per time point).

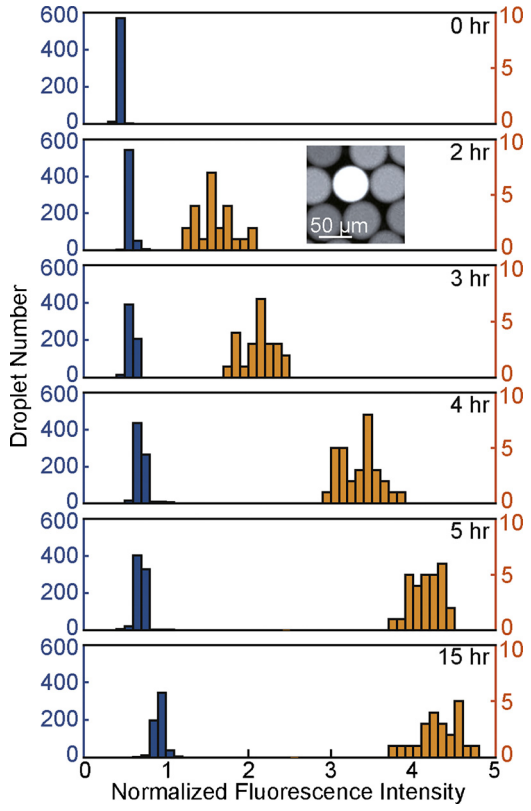

Fig. 2. The distribution of alamarBlue fluorescence intensity from drops generated from a sample containing a mixture of AmpS and AmpR cells at a ratio of [AmpS]:[AmpR] = 1:1 after incubating with 50 μg/mL of ampicillin and then with alamarBlue for different incubation times. The left axis is for the data represented in blue bars, and the right axis is for the data represented in orange bars. The inset shows a fluorescence image of droplets after 2 h of incubation with alamarBlue. The center droplet contained AmpR, and had a higher level of fluorescence than other drops. (For interpretation of the references to color in this figure legend, the reader is referred to the web version of this article.)

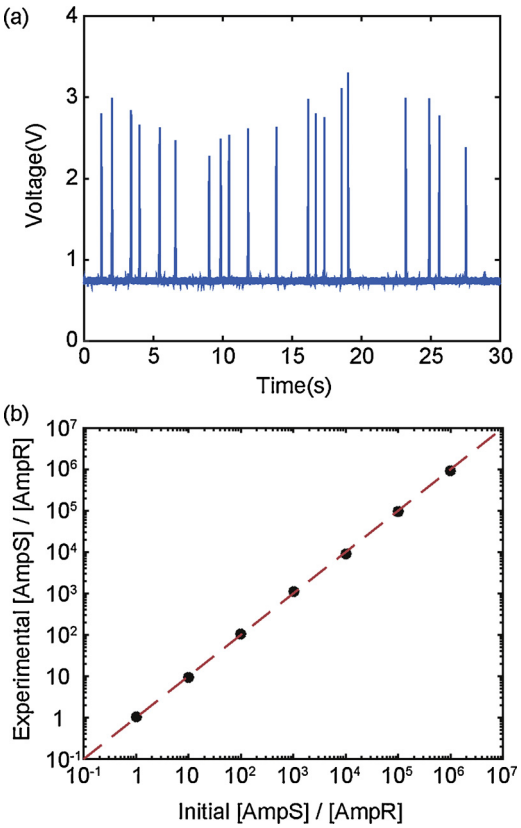

Fig. 3. Measurement of the ratio of AmpS to AmpR using microfluidic droplets. (a) Representative readout from the photomultiplier tube (PMT) using drops generated from a sample containing a mixture of AmpS and AmpR cells at a ratio of [AmpS]/[AmpR] = 1000 at a total bacteria concentration of 10^7 cfu/mL after 1 h of incubation in ampicillin followed by 2 h of incubation in alamarBlue. (b) The measured [AmpS]/[AmpR] versus the input [AmpS]/[AmpR]. Table S2 lists the values plotted.

3.3. Characterization of the resolution of the method

In order to detect a small proportion of AmpR within the bacterial sample, it is necessary to count a large number of drops. To that end, we reinjected the drops into a tapered channel containing a constriction which could fit only one drop at a time. The fluorescence from the drops was collected using a photomultiplier (PMT). Fig. 3a shows a representative voltage output from the PMT. The voltage peaks corresponded to a fluorescent drop. The signal-to-noise ratio (the ratio of the voltage corresponding to a fluorescent drop to the voltage corresponding to a non-fluorescent drop) was higher than the signal-to-noise ratio obtained from Fig. 2 (the ratio of the intensity corresponding to a fluorescent drop to the intensity corresponding to a non-fluorescent drop) due to the different optical setup used, including the use of a microscope objective with a higher magnification and numerical aperture (see Experimental Design for details). Based on the voltage output, the number of AmpR cells can then be estimated from Poisson statistics:

$$N_{AmpR} = Nln\left(\frac{N}{N - N_+}\right) \tag{1}$$

where N_+ is the number of fluorescent drops and N is the total number of drops used. Although we could not differentiate drops containing no cells from drops containing AmpS, the knowledge of the total cell concentration in the initial bacteria sample (C_0), droplet volume (V) and the total number of drops used allows us to calculate the ratio of AmpS to AmpR:

$$\frac{[AmpS]}{[AmpR]} = \frac{C_0 NV - N_{AmpR}}{N_{AmpR}} \tag{2}$$

Fig. 3b shows the measured [AmpS]/[AmpR] using our microfluidic method as a function of the input [AmpS]/[AmpR] as prepared in the bacteria sample. As can be seen, our method was accurate over 6 orders of magnitude for [AmpS]/[AmpR] = 10^6 to 1. This result verified that our method for quantifying heteroresistance is capable of identifying a resistant sub-population constituting as low as 10^{-6} of the entire cell population. This resolution is currently limited by the number of drops or cells we chose to interrogate, and practically limited by the time needed to interrogate the drops in a serial manner. This resolution can be further improved by counting an increased number of cells, and by leveraging parallel interrogation of drops to decrease the time needed to process a large number of drops [48].

3.4. Detection of the emergence of heteroresistance arising from the exposure to sub-lethal dosage of antibiotics

The high resolution of our method allows us to track the emergence of heteroresistance not possible using conventional methods. Previously, it was found that the exposure to sub-lethal antibiotic dosage increased mutation rate and antibiotic resistance in an initially susceptible strain of *E. coli* [5]. Specifically, the exposure of a homogeneous population of cells to sub-MIC dosage of ampicillin for 5 days led to a heterogeneous increase in the MIC towards ampicillin by counting 44 ampicillin-treated colonies. The resolution was intrinsically limited by the number of isolates that can be counted manually. The

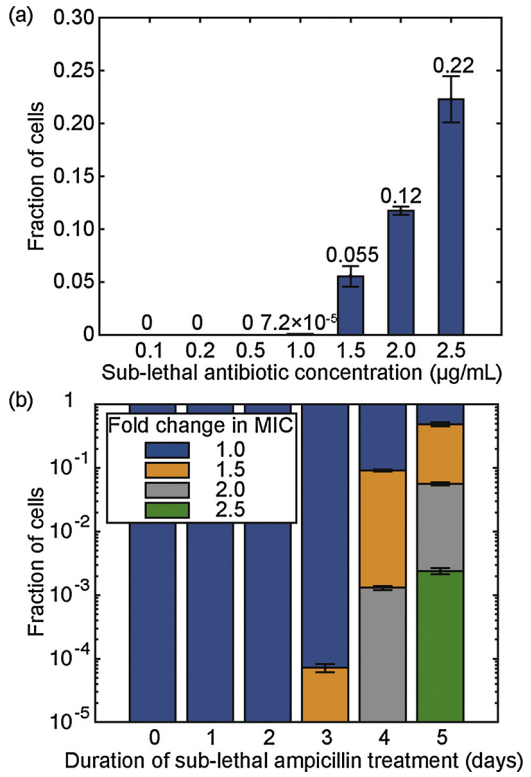

Fig. 4. (a) Fraction of cells with MIC higher than 5 μg/mL after exposing AmpS to different sub-lethal concentrations of ampicillin (0.1 μg/mL, 0.2 μg/mL, 0.5 μg/mL, 1.0 μg/mL, 1.5 μg/mL, 2.0 μg/mL, 2.5 μg/mL) for 3 days. The initial MIC was 5 μg/mL. (b) MIC distribution of ampicillin measured by the microfluidic method after exposing AmpS to 1 μg/mL ampicillin for different number of days. The height of the error bar represents one standard deviation from the mean from three separate measurements. The number of cells counted in each experiment was $> 5 \times 10^6$. We note that the MIC represented here is that of single cells. See text for details.

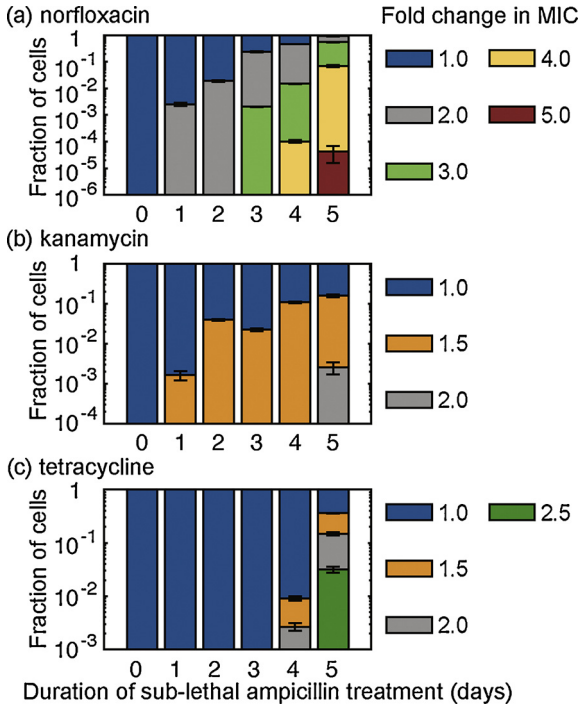

Fig. 5. MIC distribution of (a) norfloxacin, (b) kanamycin, (c) tetracycline, measured by the microfluidic method after exposing AmpS to 1 μg/mL ampicillin for 0–5 days. The initial MICs (ensemble-averaged) for norfloxacin, kanamycin, and tetracycline are 0.1 μg/mL, 5 μg/mL, 1 μg/mL respectively.

resolution was only 1/44, or 0.023. In other words, if less than 0.023 of the population exhibited resistance, it would be difficult to detect such heteroresistance using this method. In addition, this method was time-consuming. To identify the MIC, it required 24 h to allow sufficient cell growth for the optical density at 600 nm (OD_{600}) of the culture to be measurable. With such limited resolution and long time requirement for each measurement, it would be very challenging to pinpoint when heteroresistance started to emerge, or to identify the lowest dosage that can select for resistance [6].

Here, we show that we can address both challenges by using our microfluidic method. We tested our method on the effect of exposure of a single colony of AmpS to different sub-lethal dosages of ampicillin. The ensemble-average MIC of the initial AmpS culture was measured separately to be 5 μg/mL. For each droplet experiment here, we counted $> 5 \times 10^6$ cells (or $> 1.3 \times 10^7$ drops). It was thus possible to detect 1 resistant cell in 5×10^6 cells, corresponding to a resolution of 2×10^{-7}. Fig. 4a shows that an increase in MIC (exceeding 5 μg/mL) was measurable when the culture was exposed to a sub-lethal ampicillin concentration of 1 μg/mL (only 20% of the initial MIC) for 3 days. We also observed that the proportion of cells that had elevated MIC (i.e., elevated resistance) increased from 7.2×10^{-5} of the population to 0.22 of the population when the sub-lethal dosage increased from 1 μg/mL to 2.5 μg/mL. We note that the MIC represented here is a single-cell MIC: if the cell was alive after mixing with ampicillin at 5 μg/mL, we report that the cell had a MIC bigger than 5 μg/mL.

The high resolution of our measurement also enabled us to quantify the evolution of the composition of the population after exposure to sub-lethal dosage for different number of days. In Fig. 4b, we selected the lowest dosage of ampicillin (1 μg/mL) where heteroresistance was observed after 3 days, and measured the evolution of heteroresistance after cells were exposed to this dosage for 1–5 days. Here, the drops contained single cells extracted from the culture that has been exposed to different days of ampicillin at 1 μg/mL. Each drop also contained ampicillin at concentrations of 5, 7.5, or 10 μg/mL. To calculate the fraction of cells that was inhibited by the concentration of m μg/mL ampicillin, x_m, we used Eq. (3);

$$x_m = 1 - \frac{N_m}{N_c} \tag{3}$$

where N_m is the number of detected living cells after the incubation with m μg/mL ampicillin, and N_c is the number of total input cells. The number of live cells N_m is calculated from detected fluorescent drops using Eq. (1), while the number of input cells N_c is estimated by multiplying input bacterial concentration with total volume of the disperse phase. As seen in Fig. 4b, we started observing the emergence of a resistant sub-population with a 1.5-fold increase in MIC (between 5–7.5 μg/mL) after 3 days, consistent with the results in Fig. 4a. As the exposure increased to 5 days, the fraction of the resistant sub-population (cells with MIC > 5 μg/mL) reached almost half of the entire population.

Our method also enables us to compare the MIC distribution of norfloxacin, kanamycin, and tetracycline after AmpS was exposed to 1 μg/mL ampicillin for 5 days. The ensemble-average MICs of norfloxacin, kanamycin, and tetracycline for the initial AmpS colony were 0.1 μg/mL, 5 μg/mL, and 1 μg/mL, respectively. As shown in Fig. 5, after 5 days of sub-lethal ampicillin treatment, > 0.9 of the population had an increase in the MIC of norfloxacin, while only < 0.2 of the population had the elevated MIC of kanamycin.

Although we did not probe the detailed mechanism of heteroresistance here, our results are consistent the mechanism described previously that the exposure to sub-lethal dosage of antibiotics increases ROS formation and the rate of mutagenesis leading to increased resistance [5]. The increase in the proportion of resistant sub-

population as a function of sub-lethal dosage of ampicillin also agrees with previous work [8,49,50]. Our results clearly indicate that the cross-protective mechanism evoked by sub-lethal ampicillin treatment has different protective effects against other antibiotics. These results are expected since the mechanisms by which these antibiotics inactivate bacteria are different: norfloxacin inactivates bacteria by interfering with DNA replication, whereas kanamycin and tetracycline inhibit protein synthesis. In addition, despite kanamycin and tetracycline are both protein synthesis inhibitors, kanamycin and tetracycline have different modes of action and can lead to different responses from cells exposed to sub-lethal ampicillin treatment. More specifically, kanamycin interacts with the 30S ribosomal subunit resulting in mistranslation and prevents translocation during protein synthesis. On the other hand, tetracycline binds to the 16S portion of the 30S ribosomal subunit, and prevents amino-acyl tRNA to attach at A-site of mRNA-ribosome complex, thereby inhibiting protein synthesis and cell growth [51]. Further work will be needed to elucidate the precise mechanisms of the phenomena observed here; this would entail, for example, determining changes in global protein synthesis as a result of sub-lethal ampicillin treatment. A detailed investigation of this or other possible mechanisms is beyond the scope of this paper.

The key advantage of our method is the ability to resolve the heterogeneous response of the population that cannot be extracted from previous methods. In addition, our method only requires ~4 h (including droplet generation, incubation with ampicillin, pico-injection, incubation with alamarBlue and interrogation) to reveal the distribution of heteroresistance. This time can be further shortened if we had employed parallel droplet generation and interrogation methods. Nevertheless, the 4 h was already 5 times shorter than that needed for the conventional method for measuring ensemble-average MIC which requires ~ 20 h (Fig. S4) [45]. As a comparison, we verified that no increase in MIC could be measured using the conventional method for measuring ensemble-average MIC within 4 h, as OD_{600} for the culture was too low (Fig. S5). Even an increase in MIC was measurable after 20 h, the ensemble-average method cannot quantify the composition of the population. The increase in MIC could have originated from a uniform increase in MIC for all cells, or only a heterogeneous increase in MIC for only some cells as a sub-population acquires resistance. Finally, compared with genotypic approaches, our phenotypic approach is unbiased since it does not require the knowledge of all genotypic or epigenetic determinants of resistance, the identification of which is still an active area of research. While genotypic approaches can only provide binary information (either the presence or absence of resistant variant), our phenotypic approach can provide additional information on the distribution of inhibitory concentrations for the population.

3.5. Effect of gene rpoS on the emergence of heteroresistance during sub-lethal antibiotic treatment

With the ability to quantify MIC distribution in a large population of cells and detect minority variants sensitively, our method can be used to compare the emergence of heteroresistance in different cell types at the single cell level and study how genetics are linked to phenotypical differences in MIC. Specifically, for two cell types whose genetic difference is known, the difference in MIC distribution between the cell types can reveal the role of their genetic difference in the development of antibiotic resistance. To demonstrate the use of our method towards mechanistic studies, here we used wildtype *E. coli* strain "WT" and its isogenic *rpoS* deletion mutant "Δ*rpoS*" as model bacteria. The *rpoS* gene encodes sigma factor-38 (σ^{38}), which is the master regulator of the general stress response in *E. coli* [52].

In this work, we treated WT and Δ*rpoS* with sub-lethal dose of ampicillin (1 μg/mL) for 5 days, and determined the MIC change among the populations every day during the antibiotic treatment. For both untreated WT and Δ*rpoS* cells, the ensemble-average MICs of ampicillin, norfloxacin, and kanamycin were 5 μg/mL, 0.1 μg/mL, and 10 μg/mL, respectively. Fig. 6 shows that WT had an elevated MIC of ampicillin and norfloxacin after a single day of sub-lethal antibiotic treatment, while Δ*rpoS* had an elevated MIC of ampicillin and norfloxacin only after 3 days of treatment. The higher rate of antibiotic resistance development in WT than in Δ*rpoS* is consistent with previous study which showed that sub-inhibitory ampicillin treatment increased the

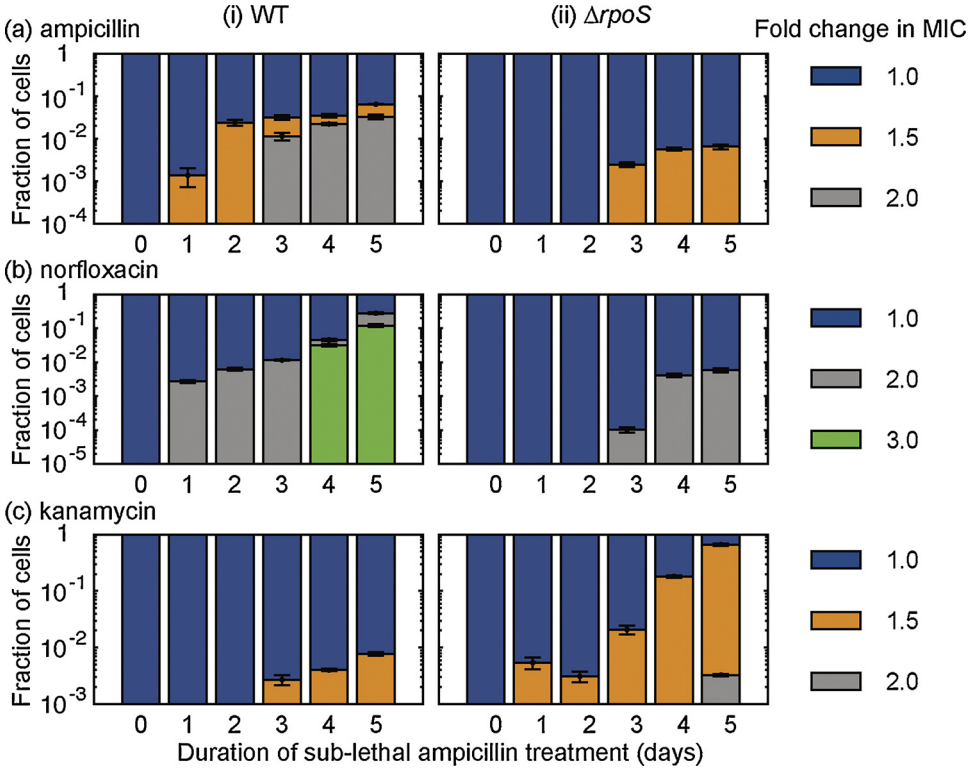

Fig. 6. MIC distribution of (a) ampicillin, (b) norfloxacin, and (c) kanamycin measured by the microfluidic method after exposing (i) WT and (ii) Δ*rpoS* to 1 μg/mL ampicillin for different number of days. For both untreated WT and Δ*rpoS* cells, the ensemble-average MICs of ampicillin, norfloxacin, and kanamycin were 5 μg/mL, 0.1 μg/mL, and 10 μg/mL, respectively.

expression of σ^{38} in WT, inducing higher mutation frequency in WT than in Δ*rpoS* [53]. The higher mutation frequency would increase the probability of adaptive mutations and cause a faster resistance development in WT than in Δ*rpoS*. On the other hand, Fig. 6c shows that the rate of kanamycin resistance development was slower in WT than in Δ*rpoS*. After 5 days of sub-lethal antibiotic treatment, we observed that the proportions of WT and Δ*rpoS* cells that had elevated MIC of kanamycin were 7.8×10^{-3} and 0.66 of the population, respectively.

In general, these results for ampicillin were as expected, as stress response-induced mutagenesis is thought to be important in the development of antibiotic resistance, and Δ*rpoS* strains have less stress response and therefore slower mutation rates [28]. However, the converse result with kanamycin was unexpected. The stress response regulated by *rpoS* is complex, and it is possible that mutations in cell wall synthesis (ampicillin target) and protein synthesis (kanamycin target) emerge differentially in the setting of stress-mediated mutagenesis. Additional work is needed to better understand the molecular basis of this interesting, differential result.

Nevertheless, this example illustrates that emergence of heteroresistance is a complex phenomenon with many unanswered mechanistic questions, for which this highly sensitive tool can be used for better characterization. The high resolution of our method enables the early distinction between WT and Δ*rpoS* when the fraction of resistant cells was as low as 10^{-4} (e.g., on day 3 in Fig. 6b(ii)). This onset time would have been missed using conventional methods with lower resolution (e.g., digital PCR has a resolution of 10^{-3} only). Both the accurate detection of the onset time of heteroresistance, as well as the precise composition of the population will be critical for follow-on investigations to elucidate the fundamental mechanisms and quantitative modeling of the evolution of heteroresistance. Such understanding could yield new insights into the relationship between genotype and phenotype as well as the mechanisms and pace of heteroresistance emergence, which could in turn inform antibiotic treatment strategies for minimizing the risk of resistance emergence during therapy.

4. Conclusions

In this work, we have demonstrated: 1) the rapid phenotyping of ABR at single cell level using droplet microfluidics, and 2) the ability to quantify heteroresistance with a resolution as low as 10^{-6} of the entire population. This high resolution enables the early detection of emergence of heteroresistance arising from the exposure of cells to a sublethal dosage of antibiotics. While this work has focused on the phenotyping of single cells, it is possible to integrate our method with the sorting and subsequent sequencing of phenotypically resistant cells to map the phenotypic behavior to the underlying genotypic patterns.

While prior work has described use of droplet microfluidics for detecting antibiotic resistance, none of it reported the measurement of heteroresistance and its evolution. In terms of the process flow of the assay, we separated the process of antibiotics incubation from the process of alamarBlue incubation to allow independent control of the two steps. The separation of these two steps was not reported in prior work, and was enabled by pico-injection of alamarBlue into drops that already contained cells and antibiotics. Finally, the use of amphiphilic nanoparticles instead of conventional surfactants as droplet stabilizer was also a new feature in our work. The use of nanoparticles mitigated the leakage of alamarBlue from drops, and allowed accurate measurement of live cells using alamarBlue.

Fundamentally, the high resolution of our method, combined with the speed we can perform the measurement, will ultimately enable the elucidation of the details of when and how heteroresistance evolves under different conditions. It will also lay the foundation for mathematical models to predict the mechanism of heteroresistance. Such understanding will in turn inform the best practices for the use of antibiotics in a variety of settings from agriculture and aquaculture to disease management. Clinically, the ability to quantify the composition of a heterogeneous population of resistant and susceptible cells is powerful, as it can inform therapeutic decisions that may be more appropriate than that based on an ensemble-average MIC alone. Our method thus holds the potential to improve patient outcomes and avert selective pressure for the emergence of resistant bacterial populations.

Acknowledgements

We acknowledge funding from the Stanford Bio-X Program, NSF Award # 1454542, and the Stanford Catalyst for Collaborative Solutions. S.T. acknowledges additional support from 3 M Untenured Faculty Award. F. L. acknowledges additional supports from the National Institute of Standards and Technology and Schlumberger Foundation Faculty for the Future.

Appendix A. Supplementary data

Supplementary data associated with this article can be found, in the online version, at https://doi.org/10.1016/j.snb.2018.05.047.

References

[1] Centers for Disease Control and Prevention, Antibiotic Resistance Threats in the United States, Centres for Disease Control and Prevention, US Department of Health and Human Services, 2013, p. 2013.
[2] V.I. Band, E.K. Crispell, B.A. Napier, C.M. Herrera, G.K. Tharp, K. Vavikolanu, et al., Antibiotic failure mediated by a resistant subpopulation in Enterobacter cloacae, Nat. Microbiol. 1 (2016) 16053.
[3] O.M. El-Halfawy, M.A. Valvano, Antimicrobial heteroresistance: an emerging field in need of clarity, Clin. Microbiol. Rev. 28 (2015) 191–207.
[4] M.E. Falagas, G.C. Makris, G. Dimopoulos, D.K. Matthaiou, Heteroresistance: a concern of increasing clinical significance? Clin. Microbiol. Infect. 14 (2008) 101–104.
[5] M.A. Kohanski, M.A. DePristo, J.J. Collins, Sublethal antibiotic treatment leads to multidrug resistance via radical-induced mutagenesis, Mol. Cell 37 (2010) 311–320.
[6] D.I. Andersson, D. Hughes, Microbiological effects of sublethal levels of antibiotics, Nat. Rev. Microbiol. 12 (2014) 465–478.
[7] S. Reardon, Resistance to last-ditch antibiotic has spread farther than anticipated, Nat. News (2017), http://dx.doi.org/10.1038/nature.2017.22140 (https://www.nature.com/news/resistance-to-last-ditch-antibiotic-has-spread-farther-than-anticipated-1.22140?WT.mc_id=TWT_NatureNews).
[8] E. Gullberg, S. Cao, O.G. Berg, C. Ilback, L. Sandegren, D. Hughes, et al., Selection of resistant bacteria at very low antibiotic concentrations, PLoS Path. 7 (2011) e1002158.
[9] G.Q. Li, F. Quan, T. Qu, J. Lu, S.L. Chen, L.Y. Cui, et al., Sublethal vancomycin-induced ROS mediating antibiotic resistance in Staphylococcus aureus, Biosci. Rep. 35 (2015) e00279.
[10] D.J. Dwyer, P.A. Belenky, J.H. Yang, I.C. MacDonald, J.D. Martell, N. Takahashi, et al., Antibiotics induce redox-related physiological alterations as part of their lethality, Proc. Natl. Acad. Sci. U. S. A. 111 (2014) E2100–E2109.
[11] J.H. Jorgensen, M.J. Ferraro, Antimicrobial susceptibility testing: a review of general principles and contemporary practices, Clin. Infect. Dis. 49 (2009) 1749–1755.
[12] K. Churski, T.S. Kaminski, S. Jakiela, W. Kamysz, W. Baranska-Rybak, D.B. Weibel, et al., Rapid screening of antibiotic toxicity in an automated microdroplet system, Lab Chip 12 (2012) 1629–1637.
[13] J.Q. Boedicker, L. Li, T.R. Kline, R.F. Ismagilov, Detecting bacteria and determining their susceptibility to antibiotics by stochastic confinement in nanoliter droplets using plug-based microfluidics, Lab Chip 8 (2008) 1265–1272.
[14] A.M. Kaushik, K. Hsieh, L. Chen, D.J. Shin, J.C. Liao, T.H. Wang, Accelerating bacterial growth detection and antimicrobial susceptibility assessment in integrated picoliter droplet platform, Biosens. Bioelectron. 97 (2017) 260–266.
[15] D.-K. Kang, M.M. Ali, K. Zhang, S.S. Huang, E. Peterson, M.A. Digman, et al., Rapid detection of single bacteria in unprocessed blood using Integrated Comprehensive Droplet Digital Detection, Nat. Commun. 5 (2014) 5427.
[16] S. Feng, D. Tseng, D. Di Carlo, O.B. Garner, A. Ozcan, High-throughput and automated diagnosis of antimicrobial resistance using a cost-effective cellphone-based micro-plate reader, Sci. Rep. 6 (2016) 39203.
[17] R. Iino, Y. Matsumoto, K. Nishino, A. Yamaguchi, H. Noji, Design of a large-scale femtoliter droplet array for single-cell analysis of drug-tolerant and drug-resistant bacteria, Front. Microbiol. 4 (2013) 300.
[18] X. Liu, R.E. Painter, K. Enesa, D. Holmes, G. Whyte, C.G. Garlisi, et al., High-throughput screening of antibiotic-resistant bacteria in picodroplets, Lab Chip 16 (2016) 1636–1643.
[19] O.M. El-Halfawy, M.A. Valvano, Chemical communication of antibiotic resistance by a highly resistant subpopulation of bacterial cells, PLoS One 8 (2013) e68874.
[20] D.B. Folkvardsen, E. Svensson, V.O. Thomsen, E.M. Rasmussen, D. Bang, J. Werngren, et al., Can molecular methods detect 1% isoniazid resistance in Mycobacterium tuberculosis? J. Clin. Microbiol. 51 (2013) 1596–1599.

[21] S. Pholwat, S. Stroup, S. Foongladda, E. Houpt, Digital PCR to detect and quantify heteroresistance in drug resistant Mycobacterium tuberculosis, PLoS One 8 (2013) e57238.
[22] S.V. Superti, D.D. Martins, J. Caierao, F.D. Soares, T. Prochnow, A.P. Zavascki, Indications of carbapenem resistance evolution through heteroresistance as an intermediate stage in acinetobacter baumannii after carbapenem administration, Rev. Inst. Med. Trop. São Paulo 51 (2009) 111–113.
[23] X.B. Zhang, B. Zhao, L.G. Liu, Y.F. Zhu, Y.L. Zhao, Q. Jin, Subpopulation analysis of heteroresistance to fluoroquinolone in Mycobacterium tuberculosis isolates from Beijing, China, J. Clin. Microbiol. 50 (2012) 1471–1474.
[24] S. Suzuki, T. Horinouchi, C. Furusawa, Prediction of antibiotic resistance by gene expression profiles, Nat. Commun. 5 (2014) 5792.
[25] A.C. Palmer, R. Kishony, Understanding, predicting and manipulating the genotypic evolution of antibiotic resistance, Nat. Rev. Genet. 14 (2013) 243–248.
[26] M. Adam, B. Murali, N.O. Glenn, S.S. Potter, Epigenetic inheritance based evolution of antibiotic resistance in bacteria, BMC Evol. Biol. 8 (2008) 52.
[27] M. Pan, M. Kim, L. Blauch, S.K.Y. Tang, Surface-functionalizable amphiphilic nanoparticles for Pickering emulsions with designer fluid–fluid interfaces, RSC Adv. 6 (2016) 39926–39932.
[28] J.H. Wang, R. Singh, M. Benoit, M. Keyhan, M. Sylvester, M. Hsieh, et al., Sigma S-dependent antioxidant defense protects stationary-phase Escherichia coli against the bactericidal antibiotic gentamicin, Antimicrob. Agents Chemother. 58 (2014) 5964–5975.
[29] D.M. Yajko, J.J. Madej, M.V. Lancaster, C.A. Sanders, V.L. Cawthon, B. Gee, et al., Colorimetric method for determining MICs of antimicrobial agents for Mycobacterium-tuberculosis, J. Clin. Microbiol. 33 (1995) 2324–2327.
[30] Y.N. Xia, G.M. Whitesides, Soft lithography, Annu. Rev. Mater. Sci. 28 (1998) 153–184.
[31] A.C. Siegel, S.K.Y. Tang, C.A. Nijhuis, M. Hashimoto, S.T. Phillips, M.D. Dickey, et al., Cofabrication: a atrategy for building multicomponent microsystems, Acc. Chem. Res. 43 (2010) 518–528.
[32] S.L. Anna, N. Bontoux, H.A. Stone, Formation of dispersions using flow focusing in microchannels, Appl. Phys. Lett. 82 (2003) 364–366.
[33] M. Pan, L. Rosenfeld, M. Kim, M. Xu, E. Lin, R. Derda, et al., Fluorinated Pickering emulsions impede interfacial transport and form rigid interface for the growth of anchorage-dependent cells, ACS Appl. Mater. Interfaces 6 (2014) 21446–21453.
[34] M. Pan, F. Lyu, S.K.Y. Tang, Fluorinated Pickering emulsions with nonadsorbing interfaces for droplet-based enzymatic assays, Anal. Chem. 87 (2015) 7938–7943.
[35] D.J. Collins, A. Neild, A. deMello, A.Q. Liu, Y. Ai, The Poisson distribution and beyond: methods for microfluidic droplet production and single cell encapsulation, Lab Chip 15 (2015) 3439–3459.
[36] S. Moon, E. Ceyhan, U.A. Gurkan, U. Demirci, Statistical modeling of single target cell encapsulation, PLoS One 6 (2011) e21580.
[37] H. Lu, O. Caen, J. Vrignon, E. Zonta, Z. El Harrak, P. Nizard, et al., High throughput single cell counting in droplet-based microfluidics, Sci. Rep. 7 (2017) 1366.
[38] A. Huebner, M. Srisa-Art, D. Holt, C. Abell, F. Hollfelder, A.J. Demello, et al., Quantitative detection of protein expression in single cells using droplet microfluidics, Chem. Commun. (2007) 1218–1220.
[39] E. Brouzes, M. Medkova, N. Savenelli, D. Marran, M. Twardowski, J.B. Hutchison, et al., Droplet microfluidic technology for single-cell high-throughput screening, Proc. Natl. Acad. Sci. U. S. A. 106 (2009) 14195–14200.
[40] S. Koster, F.E. Angile, H. Duan, J.J. Agresti, A. Wintner, C. Schmitz, et al., Drop-based microfluidic devices for encapsulation of single cells, Lab Chip 8 (2008) 1110–1115.
[41] J. Clausell-Tormos, D. Lieber, J.C. Baret, A. El-Harrak, O.J. Miller, L. Frenz, et al., Droplet-based microfluidic platforms for the encapsulation and screening of mammalian cells and multicellular organisms, Chem. Biol. 15 (2008) 427–437.
[42] A.R. Abate, T. Hung, P. Mary, J.J. Agresti, D.A. Weitz, High-throughput injection with microfluidics using picoinjectors, Proc. Natl. Acad. Sci. U. S. A. 107 (2010) 19163–19166.
[43] M. Pan, F. Lyu, S.K. Tang, Methods to coalesce fluorinated Pickering emulsions, Anal. Methods 9 (2017) 4622–4629.
[44] M. Rhee, Y.K. Light, S. Yilmaz, P.D. Adams, D. Saxena, R.J. Meagher, et al., Pressure stabilizer for reproducible picoinjection in droplet microfluidic systems, Lab Chip 14 (2014) 4533–4539.
[45] I. Wiegand, K. Hilpert, R.E.W. Hancock, Agar and broth dilution methods to determine the minimal inhibitory concentration (MIC) of antimicrobial substances, Nat. Protoc. 3 (2008) 163–175.
[46] Y. Chen, A.W. Gani, S.K.Y. Tang, Characterization of sensitivity and specificity in leaky droplet-based assays, Lab Chip 12 (2012) 5093–5103.
[47] J. Myung, M. Kim, M. Pan, C.S. Criddle, S.K.Y. Tang, Low energy emulsion-based fermentation enabling accelerated methane mass transfer and growth of poly(3-hydroxybutyrate)-accumulating methanotrophs, Bioresour. Technol. 207 (2016) 302–307.
[48] M. Kim, M. Pan, Y. Gai, S. Pang, C. Han, C. Yang, et al., Optofluidic ultrahigh-throughput detection of fluorescent drops, Lab Chip 15 (2015) 1417–1423.
[49] A. Mogre, T. Sengupta, R.T. Veetil, P. Ravi, A.S.N. Seshasayee, Genomic analysis reveals distinct concentration-dependent evolutionary trajectories for antibiotic resistance in Escherichia coli, DNA Res. 21 (2014) 711–726.
[50] H. Long, S.F. Miller, C. Strauss, C. Zhao, L. Cheng, Z. Ye, et al., Antibiotic treatment enhances the genome-wide mutation rate of target cells, Proc, Natl. Acad. Sci. U. S. A. 113 (2016) E2498–E2505.
[51] K.M.I. Bashir, M.G. Cho, The effect of kanamycin and tetracycline on growth and photosynthetic activity of two chlorophyte algae, Biomed. Res. Int. 2016 (2016).
[52] R. Hengge, Proteolysis of sigma(S) (RpoS) and the general stress response in Escherichia coli, Res. Microbiol. 160 (2009) 667–676.
[53] A. Gutierrez, L. Laureti, S. Crussard, H. Abida, A. Rodriguez-Rojas, J. Blazquez, et al., ß-lactam antibiotics promote bacterial mutagenesis via an RpoS-mediated reduction in replication fidelity, Nat. Commun. 4 (2013) 1610.

Fengjiao Lyu is currently a Ph.D. student in Mechanical Engineering at Stanford University. She received her MS degree from Stanford University in 2016. Her research focuses on the application of microfluidics in biology.

Ming Pan received his M.S. and Ph.D. degrees in Materials Science and Engineering from Stanford University in 2013 and in 2017. He focused on amphiphilic nanoparticles and Pickering emulsion.

Sunita Patil is Life Science Research Professional in the Division of Infectious Diseases and Geographic Medicine at Stanford University.

Jing-Hung Wang is a Research Scientist in Microbiology and Immunology at Stanford University. He received his Ph.D. in Pharmaceutical Sciences from University of Toronto. He is working on projects concerning antimicrobial resistance and pharmacology.

A. C. Matin is a Professor of Microbiology and Immunology at Stanford University at Stanford University. He received his Ph.D. in the Department of Microbiology (1969) in the University of California, Los Angeles. He has received two times recipient of Environmental Protection Agency's Star Award in 1991 and 1995. He was elected to the Steering Committee of Stanford Medical School Senate (2008–2011) and as a Chair of Medical School Senate Task Force for Postdoctoral Affairs (2010–2011). He was elected as an Associate Fellow, American Aerospace Medical Association (2011) and Chair Reception Committee, American Aerospace Medical Association (2012). His research interests include Biology and physiology of mixotrophy, Novel mechanisms of bacterial antibiotic resistance, Role of G proteins in starvation and motility, Discovery of a new enzyme for prodrug cancer chemotherapy and its improvement, Use of extracellular vesicles (exosomes) for specific gene and drug delivery to tumors.

Jason R. Andrews is an Assistant Professor in the Division of Infectious Diseases and Geographic Medicine at Stanford University and a practicing infectious diseases physician. His laboratory aims to develop innovative approaches to the control of infectious diseases in resource-limited settings.

Sindy K.Y. Tang is an Assistant Professor of Mechanical Engineering at Stanford University. She received her B.S. degree in Electrical Engineering from California Institute of Technology in 2003, M.S. from Stanford in 2004, and Ph.D. from Harvard in Engineering Sciences in 2010. Her lab works on the fundamental understanding of fluid mechanics and mass transport in microfluidic systems, and the application of this knowledge towards problems in biology and medicine.